

# A Novel Co(II)-organic Framework with Multiple Active Sites for Selective Gas Adsorption<sup>①</sup>

SHI Cheng-Dan<sup>a, b</sup> TIAN Jia-Yue<sup>b</sup>  
JIANG Fei-Long<sup>b</sup> CHEN Qi-Hui<sup>b②</sup> HONG Mao-Chun<sup>b②</sup>

<sup>a</sup> (College of Chemistry and Materials Science, Fujian Normal University, Fuzhou 350007, China)

<sup>b</sup> (State Key Laboratory of Structural Chemistry, Fujian Institute of Research on the Structure of Matter, Chinese Academy of Sciences, Fuzhou 350002, China)

**ABSTRACT** A novel metal-organic framework [Co(BTTA)(H<sub>2</sub>O)<sub>2</sub>]<sub>n</sub> (**FJI-H24**) has been prepared from H<sub>2</sub>BTTA ligand and CoCl<sub>2</sub>, and its structure was determined by single-crystal X-ray diffraction, thermogravimetric analysis, and Fourier transform infrared spectroscopy. It has relatively narrow pores and high density of open metal ions and free Lewis base sites. Gas adsorption tests demonstrate that **FJI-H24** has moderate CO<sub>2</sub> (34.0 cm<sup>3</sup> g<sup>-1</sup>) and C<sub>2</sub>H<sub>2</sub> (53.0 cm<sup>3</sup> g<sup>-1</sup>) adsorption capacity, but displays high selectivity of CO<sub>2</sub>/N<sub>2</sub> (87) and C<sub>2</sub>H<sub>2</sub>/CH<sub>4</sub> (66) under ambient conditions (298 K, 1 atm), which may be attributed to its relatively narrow pores and polar environment. This work will provide a potential strategy for preparing practical porous metal-organic frameworks for gas adsorption and purification.

**Keywords:** metal-organic frameworks, gas adsorption, gas purification, open metal ions, Lewis base sites;

**DOI:** 10.14102/j.cnki.0254-5861.2011-2784

## 1 INTRODUCTION

Metal-organic frameworks (MOFs) are crystalline materials consisting of metal ions or clusters and organic ligands. Owing to their inherent porosity and high specific surface area, they have wide applications in many fields such as adsorption, purification, separation, sensing, catalysis and drug delivery<sup>[1-8]</sup>. It is well known that the properties of MOFs are mainly determined by their structures including pore size and chemical environment. In order to achieve satisfactory properties, chemists not only select ligands with different sizes and metal ions with specific symmetry to tailor the pores of MOFs<sup>[9, 10]</sup>, but also introduce extra functional groups into the pores of MOFs to realize corresponding applications<sup>[11-14]</sup>. Up to now, the synthesis of MOFs with suitable pore size and chemical environment for directional application is one of the hot topics in the field of materials and chemistry.

Using MOFs materials to selectively capture carbon dioxide from exhaust gas of power plants and purify high-value hydrocarbons such as acetylene has attracted considerable attentions<sup>[4, 15-18]</sup>. In order to improve the adsorption

capacity and selectivity, it is necessary to introduce open metal ions (OMS) and Lewis base sites (LBS) into the pores of MOFs. Recently, we have prepared a porous framework **FJI-H14** based on H<sub>2</sub>BTTA (H<sub>2</sub>BTTA = 2,5-di(1H-1,2,4-triazol-1-yl)terephthalic acid) ligand and Cu(NO<sub>3</sub>)<sub>2</sub>. It showed high adsorption capacity for carbon dioxide due to the unusual synergistic effect of OMS and LBS<sup>[17]</sup>, so we intend to assemble H<sub>2</sub>BTTA (Fig. 1a) with other metal ions lighter than Cu(II) ion to construct potential MOFs for carbon dioxide uptake. Herein, a novel metal-organic framework **FJI-H24** has been prepared, which has one-dimensional (1D) quadrilateral channels with high density of open metal sites and free Lewis base sites. The gas adsorption tests demonstrate that **FJI-H24** has moderate CO<sub>2</sub> (34.0 cm<sup>3</sup> g<sup>-1</sup>) and C<sub>2</sub>H<sub>2</sub> (53.0 cm<sup>3</sup> g<sup>-1</sup>) adsorption capacity and high selectivity of CO<sub>2</sub>/N<sub>2</sub> (87) and C<sub>2</sub>H<sub>2</sub>/CH<sub>4</sub> (66) under ambient conditions (298 K, 1 atm).

## 2 EXPERIMENTAL

### 2.1 Materials and methods

Received 24 February 2020; accepted 30 March 2020 (CCDC 1978964)

① This work was supported by the National Natural Science Foundation of China (21871265) and the Youth Innovation Promotion Association CAS

② Corresponding authors. E-mails: chenqh@fjirsm.ac.cn and hmc@fjirsm.ac.cn

All chemicals are purchased from commercial sources and used without further purification. Elemental analyses for C, H and N are performed on an elemental Vairo EL analyzer. Thermogravimetric (TG) analysis experiment is carried out on a Netzsch STA 449C instrument from room temperature to 900 °C under N<sub>2</sub> atmosphere at a heating rate of 10 °C min<sup>-1</sup>. Fourier transform infrared spectra are recorded in 4000~400 cm<sup>-1</sup> on a Bruker Optics VERTEX 70 FT-IR spectrophotometer with KBr pellets. The powder X-ray diffraction patterns (XRD) are recorded on a RIGAKU-DMAX2500 X-ray diffractometer using CuK $\alpha$  radiation ( $\lambda$  = 0.154184 nm). The gas sorption experiments are performed by using the Accelerated Surface Area and Porosimetry measurement 2020 system (ASAP2020), and all measurements are implemented by using extremely high purity gases N<sub>2</sub>, CO<sub>2</sub>, C<sub>2</sub>H<sub>2</sub> and CH<sub>4</sub> (> 99.999%).

## 2.2 Synthesis of FJI-H24

A mixture of anhydrous CoCl<sub>2</sub> (0.007 g, 0.05 mmol), H<sub>2</sub>BTTA (0.030 g, 0.1 mmol), DMF (2.0 mL), and H<sub>2</sub>O (0.5 mL) was added into a 20 mL high-pressure autoclave, heated at 110 °C for 72 h and cooled down to room temperature. Finally, the pink block crystals of **FJI-H24** were obtained with 80% yield. IR (KBr, cm<sup>-1</sup>): 3437, 3141, 1666, 1577, 1533, 1404, 1361, 1278, 1137, 1055, 985, 813, 651, 595 and 540. Elemental analysis calcd. (%) for **FJI-H24** (C<sub>12</sub>H<sub>10</sub>CoN<sub>6</sub>O<sub>6</sub>): C, 36.66; H, 2.56; N, 21.37. Found: C,

36.98; H, 2.29; N, 21.12%.

## 2.3 Structure determination

Single-crystal X-ray diffraction data are collected on a Super Nova diffractometer with CuK $\alpha$  radiation ( $\lambda$  = 1.54184 Å) by using the  $\omega$ -scan technique at 164.0(9) K. Data collection and reduction are measured on *CrysAlisPro* 171.37.35 software. The structure of **FJI-H24** is solved by *SHELXT* (direct methods) and refined by *SHELXL* (full-matrix least-squares techniques) in the *Olex-2* package<sup>[19]</sup>. The non-hydrogen atoms are refined anisotropically, and the hydrogen atoms of organic linker are refined isotropically as riding atoms. The guest solvents are removed through the *SQUEEZE* option of *PLATON*<sup>[20]</sup>. **FJI-H24** crystallizes in monoclinic system with space group *I2/a*,  $a$  = 11.1096(5),  $b$  = 15.5982(7),  $c$  = 16.7051(9) Å,  $\beta$  = 108.394(6)°,  $V$  = 2746.9(2) Å<sup>3</sup>,  $Z$  = 4,  $D_c$  = 0.951 g cm<sup>-3</sup>,  $F(000)$  = 796 and  $\mu$  = 5.147 mm<sup>-1</sup>. A total of 9151 reflections and 2458 unique ones ( $R_{int}$  = 0.0366) are measured in the range of  $3.98 \leq \theta \leq 67.05^\circ$ , of which 2128 with  $I > 2\sigma(I)$  are used in the succeeding refinement. The final  $R$  = 0.0590,  $wR$  = 0.1804 ( $w = 1/[\sigma^2(F_o^2) + (0.1159P)^2 + 4.9603P]$ , where  $P = (F_o^2 + 2F_c^2)/3$ ),  $(\Delta\rho)_{max}$  = 0.533,  $(\Delta\rho)_{min}$  = -0.469 e/Å<sup>3</sup>,  $(\Delta/\sigma)_{max}$  = 0.000 and  $S$  = 1.060. The final chemical formula of **FJI-H24** is deduced by the crystal data after *SQUEEZE* process. Partial bond lengths and bond angles of the structure are summarized in Table 1.

Table 1. Selected Bond Lengths (Å) and Bond Angles (°)

Bond	Dist.	Bond	Dist.	Bond	Dist.
Co(1)–O(2)	2.101(2)	Co(1)–O(1)	2.117(2)	Co(1)–N(3) <sup>b</sup>	2.119(3)
Co(1)–O(2) <sup>a</sup>	2.101(2)	Co(1)–O(1) <sup>a</sup>	2.117(2)	Co(1)–N(3) <sup>c</sup>	2.119(3)
Angle	(°)	Angle	(°)	Angle	(°)
O(2)–Co(1)–O(2) <sup>a</sup>	180.0	O(2) <sup>a</sup> –Co(1)–O(1) <sup>a</sup>	90.13(9)	O(2)–Co(1)–O(1) <sup>a</sup>	89.87(9)
O(2) <sup>a</sup> –Co(1)–O(1)	89.87(9)	O(2)–Co(1)–O(1)	90.13(9)	O(2)–Co(1)–N(3) <sup>b</sup>	88.90(10)
O(2)–Co(1)–N(3) <sup>c</sup>	91.10(10)	O(2) <sup>a</sup> –Co(1)–N(3) <sup>b</sup>	91.10(10)	O(2) <sup>a</sup> –Co(1)–N(3) <sup>c</sup>	88.90(10)
O(1)–Co(1)–O(1) <sup>a</sup>	180.0	O(1)–Co(1)–N(3) <sup>b</sup>	89.95(11)	O(1)–Co(1)–N(3) <sup>c</sup>	90.05(11)
O(1) <sup>a</sup> –Co(1)–N(3) <sup>b</sup>	90.05(11)	O(1) <sup>a</sup> –Co(1)–N(3) <sup>c</sup>	89.95(11)	N(3) <sup>b</sup> –Co(1)–N(3) <sup>c</sup>	180.0

Symmetry transformation: a: 1– $x$ , 1– $y$ , 1– $z$ ; b: –1/2+ $x$ , 1– $y$ ,  $z$ ; c: 3/2– $x$ ,  $y$ , 1– $z$

## 3 RESULTS AND DISCUSSION

### 3.1 Crystal structure description

The single-crystal X-ray diffraction shows that **FJI-H24** crystallizes in the monoclinic space group *I2/a*. Its asymmetric unit contains one Co(II) ion, one H<sub>2</sub>BTTA ligand and two water molecules. As shown in Fig. 1b, each Co(II) ion adopts an octahedral coordination geometry through coordinating with four O and two N atoms. Four positions of the equatorial

plane are occupied by two N atoms from different triazolyl groups and two O atoms from coordinated water, and two axial positions are occupied by two O atoms from different carboxyl groups. Then each Co(II) ion coordinates with neighboring BTTA<sup>2-</sup> ligands to form a three-dimensional (3D) porous framework with 1D quadrilateral channel along the  $a$  axis (Fig. 1c). Interestingly, the pore walls are densely populated with the uncoordinated N atoms from triazolyl groups and Co(II) ions with two coordinated water molecules.

After activation, such Co(II) ions will be transformed into active open Co(II) ions, generating a polar environment for gas adsorption. Such potential open Co(II) ions and neighboring free N atoms from triazolyl groups may synergistically improve the gas adsorption. Both Co(II) ions and  $\text{BTTA}^{2-}$  ligands can be considered as 4-connected nodes, so the framework of **FJI-H24** can be simplified to a 4-connected **lvt** network with the point symbol of  $(4^2.8^4)$  (Fig. 1d). Very recently, a compound with similar coordination environ-

ment has been reported, but it displays a typical two-dimensional layered structure rather than a three-dimensional porous structure<sup>[21]</sup> mainly due to the different conformation and orientation of ligands in these two compounds. The porosity of **FJI-H24** is estimated to be 50% according to *PLATON* calculation with a probe radius of 1.8 Å. Revealed by *Zeo++* software, the limiting pore diameter and the maximum pore diameter are 4.7 and 5.7 Å, respectively<sup>[22]</sup>.

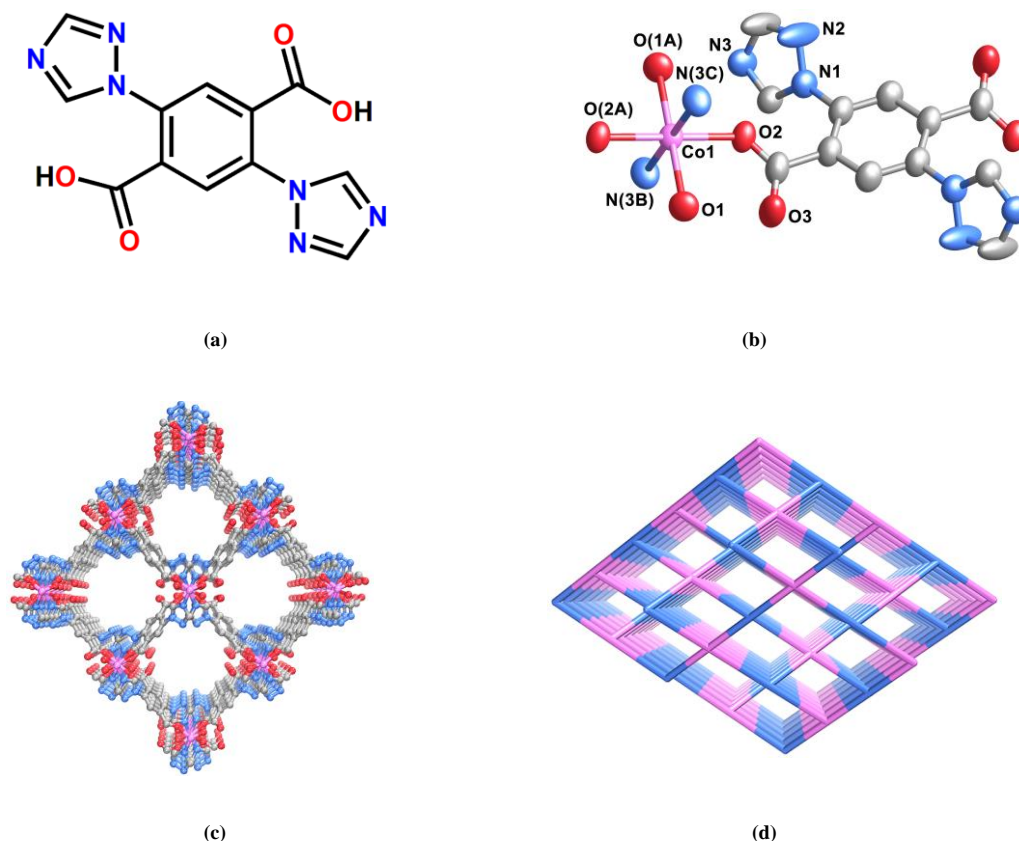


Fig. 1. (a) Structure of ligand  $\text{H}_2\text{BTTA}$ . (b) Coordination environment of Co(II) ion in **FJI-H24**.

Symmetry codes: A:  $1-x, 1-y, 1-z$ ; B:  $-1/2+x, 1-y, z$ ; C:  $3/2-x, y, 1-z$ ;

(c) Framework of **FJI-H24**. (d) Topology of **FJI-H24**

### 3.2 PXRD, TGA and FT-IR analyses

As shown in Fig. S1a, the Powder X-ray diffraction (PXRD) patterns of the as-synthesized sample match well with the simulated one, indicating that the bulk as-synthesized **FJI-H24** sample is pure. The framework of **FJI-H24** remains stable after soaking in acetone, which reveals that acetone can be used to exchange free solvents inside the pores of **FJI-H24**. Thermogravimetric analyses (TGA) demonstrate that both free water and N,N-dimethylformamide molecules are comprised in **FJI-H24** and its framework can be thermally stable up to about 250 °C (Fig. S1b). Fourier transform infrared spectra (FT-IR) analyses further prove the existence

of free water and N,N-dimethylformamide molecules, in which the broad peak of  $3437\text{ cm}^{-1}$  belongs to water molecule and the strong peak of  $1666\text{ cm}^{-1}$  attributes to the N,N-dimethylformamide (Fig. S1c).

### 3.3 Gas storage and purification

As mentioned above, the **FJI-H24** not only has typical micro-porous structure, but also has high density of metal ions and uncoordinated N atoms; both of them are beneficial to carbon dioxide adsorption. Before adsorption test, the fresh sample **FJI-H24** should be soaked in acetone for 3 days to remove less volatile solvents, and activated under dynamic vacuum at 60 °C for 12 h. PXRD data indicate that the

framework of desolvated **FJI-H24** (after activation) is retained. The permanent porosity of **FJI-H24** is firstly tested by  $N_2$  adsorption measurement at 77 K; however, no obvious  $N_2$  adsorption at 77 K has been observed. Such almost zero  $N_2$  adsorption at 77 K may result from the relatively narrow pores in **FJI-H24** and their polar environment; both narrow pores and polar environment will hinder the diffusion of  $N_2$  (the kinetic diameter of  $N_2$  molecule is 3.6 Å) into pores of **FJI-H24** at 77 K. Thus, the permanent porosity of **FJI-H24** is tested by  $CO_2$  adsorption at 195 K. As shown in Fig. 2a, the  $CO_2$  sorption isotherm at 195 K exhibits a type-I microporous isotherm with a saturated adsorption of about  $84 \text{ cm}^3 \text{ g}^{-1}$ . The Brunauer-Emmett-Teller (BET) and Langmuir surface areas are 259 and  $294 \text{ m}^2 \text{ g}^{-1}$ , respectively. To check the  $CO_2$  capture capacity of **FJI-H24** at ambient conditions,  $CO_2$  sorption isotherms are further tested at 273 and 298 K, respectively. The  $CO_2$  uptake at 273 K is about  $42.7 \text{ cm}^3 \text{ g}^{-1}$ , and its value will reduce to  $34.0 \text{ cm}^3 \text{ g}^{-1}$  when the temperature rises to 298 K (Fig. 2b). Compared with **FJI-H14** (the  $CO_2$  capture capacity of **FJI-H14** is about  $171 \text{ cm}^3 \text{ g}^{-1}$  at 298 K and 1 atm), the  $CO_2$  adsorption capacity of **FJI-H24** is significantly reduced, which may attribute to its more narrow

pores and lower BET surface areas than that of **FJI-H14**. For comparison,  $N_2$  sorption isotherms at different temperature are also measured; corresponding  $N_2$  uptake is only 3.9 and  $2.5 \text{ cm}^3 \text{ g}^{-1}$ , separately. According to the ideal absorbed solution theory (IAST), the  $CO_2/N_2$  selectivity for the  $CO_2/N_2$  (15/85) mixture at 1 atm is about 87 at 298 K (Fig. 3a), exceeding that of **FJI-H14** (the  $CO_2/N_2$  selectivity of **FJI-H14** is 51)<sup>[17]</sup> and many recently reported MOF, such as **HBU-18** (the  $CO_2/N_2$  selectivity of **HBU-18** is 41.79)<sup>[23]</sup> and **Cu-BTC/GO10** (the  $CO_2/N_2$  selectivity of **Cu-BTC/GO10** is 28.1)<sup>[24]</sup>. The relatively high  $CO_2/N_2$  selectivity of **FJI-H24** may result from its polar environment which can interact with polar  $CO_2$  molecule strongly. To evaluate the interactions between the framework and  $CO_2$  molecules, the isosteric heat of adsorption (Qst) of **FJI-H24** has been calculated from their adsorption isotherms at 273 and 298 K based on the Clausius-Clapeyron equation. As shown in Fig. 3b, the Qst value at the onset of adsorption is  $24.46 \text{ kJ mol}^{-1}$ . Such relatively high  $CO_2/N_2$  selectivity demonstrates that **FJI-H24** is a potential adsorbent for the removal of carbon dioxide from exhaust gas of power plants.

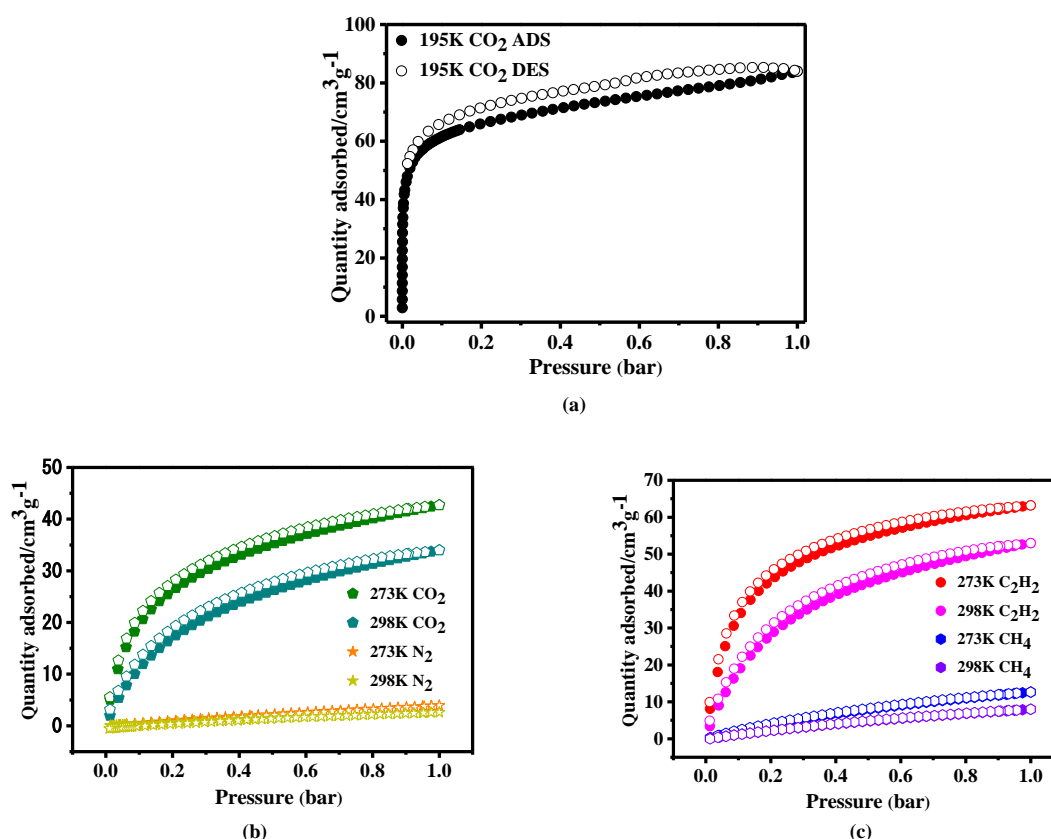


Fig. 2. (a)  $CO_2$  adsorption isotherms of **FJI-H24** at 195 K. (b)  $CO_2$  and  $N_2$  adsorption isotherms of **FJI-H24** at 273 and 298 K. (c)  $C_2H_2$  and  $CH_4$  adsorption isotherms of **FJI-H24** at 273 and 298 K

Acetylene is a very significant chemical material in industry, which can be used for manufacturing synthetic rubber, synthetic fiber, etc. However, the safe storage of acetylene still remains a big challenge due to its explosiveness<sup>[4]</sup>. Considering that the kinetic diameter of  $C_2H_2$  is the same as  $CO_2$  (3.3 Å), **FJI-H24** may be a potential adsorbent for  $C_2H_2$ , so  $C_2H_2$  sorption measurements for **FJI-H24** are also carried out. As shown in Fig. 2c, the  $C_2H_2$  uptake at 273 K is about  $63.2\text{ cm}^3\text{ g}^{-1}$ , and its value at 298 K is about  $53.0\text{ cm}^3\text{ g}^{-1}$ . Acetylene is usually prepared by partial oxidation of methane in industry, so removing unreacted methane from acetylene is very important. A practical  $C_2H_2$  adsorbent usually requires excellent  $C_2H_2/CH_4$  selectivity. For comparison,  $CH_4$  sorption isotherms are measured at 298 and 273

$\text{cm}^3\text{ g}^{-1}$ , separately. Excitedly, the  $C_2H_2/CH_4$  selectivity at ambient conditions (298 K, 1 atm) is up to 66 (Fig. 3a). To the best of our knowledge, the selectivity of  $C_2H_2/CH_4$  exceeds many recently reported MOFs under the same condition, such as ZJNU-100 (22.2)<sup>[25]</sup> and Sc-ABTC (14.7)<sup>[26]</sup>. The isosteric heat of adsorption ( $Q_{st}$ ) also has been calculated based on their adsorption isotherms at 273 and 298 K. At near zero loading, the  $Q_{st}$  of **FJI-H24** for  $C_2H_2$  is about  $22.30\text{ kJ mol}^{-1}$  (Fig. 3b). Such moderate  $C_2H_2$  adsorption performance and high  $C_2H_2/CH_4$  selectivity may also result from the relatively narrow pores and high density of free N atoms and open metal ions comprised of **FJI-H24**, which indicates that **FJI-H24** is a potential material for purification of raw acetylene from oxidation of methane.

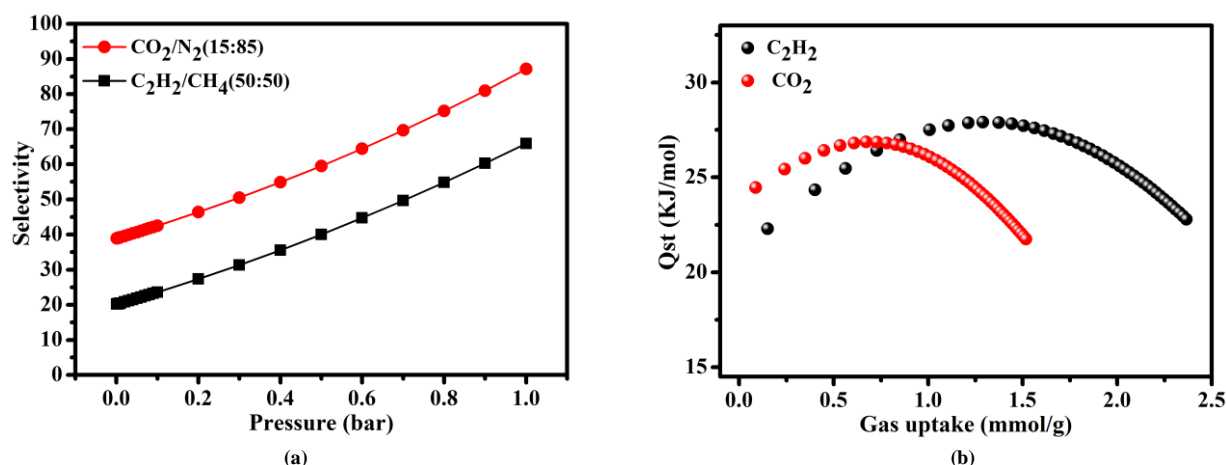


Fig. 3. (a) IAST adsorption selectivity of FJI-H24 for different gas mixtures at 1 atm and 298 K.

(b) Isostatic heat of adsorption of  $CO_2$  and  $C_2H_2$  for FJI-H24

#### 4 CONCLUSION

In conclusion, a novel metal-organic framework **FJI-H24** with narrow pores and high density of open metal ions and free Lewis base sites has been prepared from  $H_2BTTA$  ligand and  $CoCl_2$ . **FJI-H24** has moderate  $CO_2$  ( $34.0\text{ cm}^3\text{ g}^{-1}$ ) and  $C_2H_2$  ( $53.0\text{ cm}^3\text{ g}^{-1}$ ) adsorption capacity, but displays

relatively high  $CO_2/N_2$  (87) and  $C_2H_2/CH_4$  (66) selectivity under ambient conditions (298 K, 1 atm). The relationship between adsorption and structure has been discussed in detail, which will provide a potential strategy for preparing practical porous metal-organic frameworks for gas adsorption and purification.

#### REFERENCES

- (1) Trickett, C. A.; Popp, T. M. O.; Su, J.; Yan, C.; Weisberg, J.; Huq, A.; Urban, P.; Jiang, J.; Kalmutzki, M. J.; Liu, Q.; Baek, J.; Head-Gordon, M. P.; Somorjai, G. A.; Reimer, J. A.; Yaghi, O. M. Identification of the strong Bronsted acid site in a metal-organic framework solid acid catalyst. *Nat. Chem.* **2019**, 11, 170–176.
- (2) Cui, Y.; Li, B.; He, H.; Zhou, W.; Chen, B.; Qian, G. Metal-organic frameworks as platforms for functional materials. *Acc. Chem. Res.* **2016**, 49, 483–493.
- (3) Hu, Z.; Deibert, B. J.; Li, J. Luminescent metal-organic frameworks for chemical sensing and explosive detection. *Chem. Soc. Rev.* **2014**, 43, 5815–5840.

- (4) Getman, R. B.; Bae, Y. S.; Wilmer, C. E.; Snurr, R. Q. Review and analysis of molecular simulations of methane, hydrogen, and acetylene storage in metal-organic frameworks. *Chem. Rev.* **2012**, 112, 703–723.
- (5) Zhang, J. P.; Zhang, Y. B.; Lin, J. B.; Chen, X. M. Metal azolate frameworks: from crystal engineering to functional materials. *Chem. Rev.* **2012**, 112, 1001–1033.
- (6) Liang, L. F.; Jiang, F. L.; Chen, Q. H.; Yuan, D. Q.; Hong, M. C. Ultra-microporous metal-organic framework with high concentration of free carboxyl groups and Lewis basic sites for CO<sub>2</sub> capture at ambient conditions. *Chin. J. Struct. Chem.* **2019**, 38, 559–565.
- (7) Cui, P. P.; Liu, Y.; Zhai, H. G.; Zhu, J. P.; Yan, W. N.; Yang, Y. M. Two copper-organic frameworks constructed from the flexible dicarboxylic ligands. *Chin. J. Struct. Chem.* **2020**, 39, 368–374.
- (8) Li, B.; Fang, W. J.; Liu, S. Q.; Zhao, H.; Zhang, J. J. Two novel coordination polymers with (6,3) topology constructed by an imidazole-containing isophthalic ligand: syntheses, structures and luminescence properties. *Chin. J. Struct. Chem.* **2020**, 39, 110–117.
- (9) Zhang, J. P.; Zhou, H. L.; Zhou, D. D.; Liao, P. Q.; Chen, X. M. Controlling flexibility of metal-organic frameworks. *Nat. Sci. Rev.* **2018**, 5, 907–919.
- (10) Chen, K. J.; Madden, D. G.; Pham, T.; Forrest, K. A.; Kumar, A.; Yang, Q. Y.; Xue, W.; Space, B.; Perry, J. J.; Zhang, J. P.; Chen, X. M.; Zaworotko, M. J. Tuning pore size in square-lattice coordination networks for size-selective sieving of CO<sub>2</sub>. *Angew. Chem. Int. Ed.* **2016**, 55, 10268–10272.
- (11) Liao, P. Q.; Chen, H.; Zhou, D. D.; Liu, S. Y.; He, C. T.; Rui, Z.; Ji, H.; Zhang, J. P.; Chen, X. M. Monodentate hydroxide as a super strong yet reversible active site for CO<sub>2</sub> capture from high-humidity flue gas. *Energy Environ. Sci.* **2015**, 8, 1011–1016.
- (12) Xue, H.; Song, D.; Liu, C.; Lyu, G.; Yuan, D.; Jiang, F.; Chen, Q.; Hong, M. A porous framework as a variable chemosensor: from the response of a specific carcinogenic alkyl-aromatic to selective detection of explosive nitroaromatics. *Chem. Eur. J.* **2018**, 24, 11033–11041.
- (13) Xue, H.; Chen, Q.; Jiang, F.; Yuan, D.; Lv, G.; Liang, L.; Liu, L.; Hong, M. A regenerative metal-organic framework for reversible uptake of Cd(II): from effective adsorption to in situ detection. *Chem. Sci.* **2016**, 7, 5983–5988.
- (14) Liang, L.; Chen, Q.; Jiang, F.; Yuan, D.; Qian, J.; Lv, G.; Xue, H.; Liu, L.; Jiang, H. L.; Hong, M. *In situ* large-scale construction of sulfur-functionalized metal-organic framework and its efficient removal of Hg(II) from water. *J. Mater. Chem. A* **2016**, 4, 15370–15374.
- (15) Wang, Q.; Luo, J.; Zhong, Z.; Borgna, A. CO<sub>2</sub> capture by solid adsorbents and their applications: current status and new trends. *Energy Environ. Sci.* **2011**, 4, 42–55.
- (16) Xiang, S.; He, Y.; Zhang, Z.; Wu, H.; Zhou, W.; Krishna, R.; Chen, B. Microporous metal-organic framework with potential for carbon dioxide capture at ambient conditions. *Nat. Commun.* **2012**, 3, 954–9.
- (17) Liang, L.; Liu, C.; Jiang, F.; Chen, Q.; Zhang, L.; Xue, H.; Jiang, H. L.; Qian, J.; Yuan, D.; Hong, M. Carbon dioxide capture and conversion by an acid-base resistant metal-organic framework. *Nat. Commun.* **2017**, 8, 1233–10.
- (18) Pang, J.; Jiang, F.; Wu, M.; Liu, C.; Su, K.; Lu, W.; Yuan, D.; Hong, M. A porous metal-organic framework with ultrahigh acetylene uptake capacity under ambient conditions. *Nat. Commun.* **2015**, 6, 7575–7.
- (19) Dolomanov, O. V.; Bourhis, L. J.; Gildea, R. J.; Howard, J. A. K.; Puschmann, H. OLEX2: a complete structure solution, refinement and analysis program. *J. Appl. Cryst.* **2009**, 42, 339–341.
- (20) Spek, A. L. PLATON SQUEEZE: a tool for the calculation of the disordered solvent contribution to the calculated structure factors. *Acta Cryst.* **2015**, 71, 9–18.
- (21) Cai, H.; Li, N.; Zhang, N.; Yang, Z.; Cao, J.; Lin, Y.; Min, N.; Wang, J. Metal-directed supramolecular architectures based on the bifunctional ligand 2,5-bis(1H-1,2,4-triazol-1-yl)terephthalic acid. *Acta Cryst. C* **2020**, 76, 118–124.
- (22) Willems, T. F.; Rycroft, C. H.; Kazi, M.; Meza, J. C.; Haranczyk, M. Algorithms and tools for high-throughput geometry-based analysis of crystalline porous materials. *Micropor. Mesopor. Mater.* **2012**, 149, 134–141.
- (23) Liu, J. M.; Hou, J. X.; Liu, J.; Jing, X.; Li, L. J.; Du, J. Pyrazinyl-functionalized Zr(IV)-MOF for ultrasensitive detection of tyrosine/TNP and efficient CO<sub>2</sub>/N<sub>2</sub> separation. *J. Mater. Chem. C* **2019**, 7, 11851–11857.
- (24) Barbara, S.; Jerzy, C.; Graphene-containing microporous composites for selective CO<sub>2</sub> adsorption. *Microporous Mesoporous Mater.* **2020**, 292, 109761–7.
- (25) Wang, Y.; He, M.; Gao, X.; Wang, X.; Xu, G.; Zhang, Z.; He, Y. A ligand conformation preorganization approach to construct a copper-hexacarboxylate framework with a novel topology for selective gas adsorption. *Inorg. Chem. Front.* **2019**, 6, 263–270.
- (26) Zhang, J. W.; Qu, P.; Hu, M. C.; Li, S. N.; Jiang, Y. C.; Zhai, Q. G. Topology-guided design for Sc-soc-MOFs and their enhanced storage and separation for CO<sub>2</sub> and C<sub>2</sub>-hydrocarbons. *Inorg. Chem.* **2019**, 58, 16792–16799.